The calculation of the resistivity of liquid and amorphous transition metals via the Landauer formula

1995 J. Phys.: Condens. Matter 7 1543

(http://iopscience.iop.org/0953-8984/7/8/004)

J. Phys.: Condens. Matter 7 (1995) 1543–1556. Printed in the UK

The calculation of the resistivity of liquid and amorphous transition metals via the Landauer formula

René Kahnt
Fachbereich Physik, Technische Universität Chemnitz, 09009 Chemnitz, PF 964, Germany

Received 25 May 1994, in final form 21 November 1994

Abstract. Employing the concept of elastic multiple scattering, we used the Landauer/Büttiker conductance formulas for calculating resistivities of realistic structural models of strongly scattering disordered materials. Our model is based on the calculation of scattering matrices of supercells with about one hundred atoms which are arranged into a two-dimensional layer. Resistivities are obtained upon extracting the average linear dependence of the transmission on the layer thickness. The smoothing of the Fermi surface is included just as in the Kubo–Greenwood formula. We applied our method in resistivity calculations of liquid and amorphous transition metals.

1. Introduction

For many years there has been increasing interest in the theoretical description of the properties of liquid and amorphous transition metals (TMs). Today there exist several theoretical approaches for calculating electronic properties which are the foundations for an improved understanding of this kind of material. In recent years, first-principles calculations of the density of states (DOS) have been performed. These calculations are based on LKKR, LCAO, LMTO and multiple-scattering (MS) schemes and have to work self-consistently. Today systems of $\approx 10^2$ atoms can be treated in that way and the results are nearly independent of the employed approach. The starting point for all these calculations is structure models. These models are generated by molecular dynamical (MD) or Monte Carlo (MC) procedures. Much progress has been made in treating the particle interactions quantum mechanically. Unfortunately, such advanced techniques which are based on plane wave basis sets [1] cannot be used because of the resonant d states. But H–NFE–TB derived effective pair potentials work quite reasonably [2, 3]. Systems with many more than onehundred atoms have to be simulated by use of effective potentials. Alternatively, reverse Monte Carlo (RMC) procedures [4] can be used. The generated structure models are characterized by nearly the same statistical properties as structures that come from MD or MC schemes.

The special subject of our work is the DC conductivity or resistivity of these materials. Most formalisms for calculating these quantities only work for weakly scattering materials (mean free path l_f much greater than the interatomic distance $\bar{d}_{at-at}$) or dilute alloys. The most popular generalization is the extended Ziman formula. This approach does not work very well for amorphous and liquid TMs. Improved results were obtained upon employing effective valences. We believe that such approaches are not consistent, because DOS calculations also need a complete MS treatment to produce correct results. Until now, only the approaches within the linear response theory (e.g. the Kubo–Greenwood formula [5]) are able to reproduce experimental results with a good accuracy.

0953-8984/95/081543+14$19.50

Otherwise, methods for calculating the resistance of mesoscopic systems are under discussion. Aa early as 1957 the basic ideas for such calculations were published by Landauer [6]. He calculated the conductance of a one-dimensional scatterer between ideal one-channel leads as a function of its reflection (R) and transmission (T) coefficients as $G = (2e^2/h)T/R$. This is known as the one-channel Landauer formula. In connection with the explanation of quantum effects in mesoscopic systems, like conductance quantization, universal conductance fluctuations, Aharonov–Bohm effect and others this Landauer picture had a big revival. An alternative treatment of the same problem led to another one-dimensional conductance formula, the so called one-channel Büttiker formula $G = (2e^2/h)T$. Until now in a certain experimental situation, it has not been clear which formula has to be used. Furthermore, there were developed different formulas for the situation of many-channel leads, e.g. the many-channel Landauer [7] formula,

$$G = \frac{2e^2}{h}\left(\sum_i T_i \quad 2\sum_i \frac{1}{v_i}\right) \Big/ \left(\sum_i \frac{1}{v_i}(1 + R_i - T_i)\right) \tag{1}$$

and the multichannel Büttiker formula

$$G = \frac{2e^2}{h}\sum_i T_i \tag{2}$$

as generalizations of the one-channel cases. Here T_i (R_i) are the total transmission (reflection) probabilities into the ith channel. They can be calculated from the S matrix according to

$$T_i = \sum_j |S_{ij}^{\alpha\alpha}|^2 \qquad R_i = \sum_j |S_{ij}^{\alpha(-\alpha)}|^2. \tag{3}$$

Büttiker *et al* [7] have shown that (1) is the conductance of the scatterer alone, while (2) includes contributions of the ideal leads, too. Nevertheless, (2) is often used to calculate the conductances of a bare scatterer. As yet there is some lack of knowledge of how the above conductance formulas have to be applicated. This work will not attempt to answer this question. Our goal is rather to use such conductance formulas for calculating the conductivity/resistivity of realistic strongly scattering materials. Therefore, a model of an infinite disordered system is needed which can be used in multichannel conductance formulas like (1), (2).

One way to proceed may be to put a realistic cluster model into a confinement, e.g. a tube. However, in this model a large part of the scatterers is situated near the wall. The properties of these scatterers are influenced by the wall, leading to deviations from bulk properties.

Another way, the application of periodic boundary conditions in two dimensions, has the advantage that many more scatterers are situated in typical bulk surroundings. So we have to treat the transport perpendicular to a two-dimensionally periodic slab which is not periodic in the third dimension. The two-dimensional basic cell has the dimensions aa and the layer has a thickness l with $l \approx 1 \ldots 2a$. The situation is shown in figure 1. Upon adding periodicity in the third direction one gets a resistivity of zero or infinty depending on the band structure $E(\boldsymbol{k})$ of the supercrystal. Our model should be better, the smaller the mean free path is. In 3d TM systems $l_f \approx \bar{d}_{\mathrm{at-at}}$ holds. Especially the case $a \gg d_{\mathrm{at-at}}$ should simulate a bulk material.

This paper demonstrates the method for calculating the resistivity with the help of such multichannel conductance formulae. The formalism is shown in detail in [8].

In section 2 we give the basic equations for calculating the S matrix in a MS picture. The structure models and the scattering phase shifts as input of our calculations are discussed in

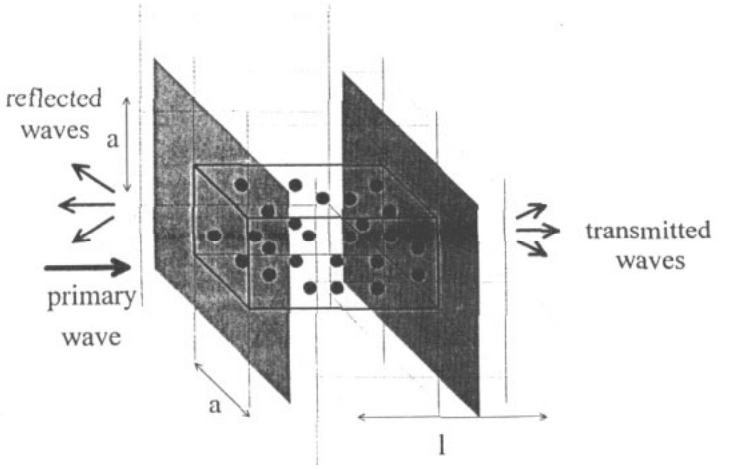

Figure 1. Two-dimensional periodic layer with a periodicity a and a thickness l. An incident plane wave is scattered into outgoing waves differing by vectors of the two-dimensional reciprocal lattice. We are interested in the transport perpendicular to this layer.

section 3. Then we show some curves which demonstrate the behaviour of our model and apply it to realistic materials. At the end we give a short discussion.

2. Theory

2.1. Basic model

The electron scattering at a two-dimensional periodic layer can be treated in a plane wave basis. The plane waves

$$\varphi_\tau^\alpha(E, \boldsymbol{k}_\parallel, \boldsymbol{r}) = \frac{1}{\sqrt{\kappa_\tau}} \exp i\boldsymbol{k}_\tau^\alpha \cdot \boldsymbol{r} \qquad \boldsymbol{k}_\tau^\alpha = \boldsymbol{k}_\parallel + \tau + \hat{\boldsymbol{e}}_z \alpha \kappa_\tau \qquad \kappa_\tau = \sqrt{\kappa^2 - (\boldsymbol{k}_\parallel + \tau)^2} \tag{4}$$

are characterized by the energy $|\kappa|^2$ and by the wave vector $\boldsymbol{k}_\parallel$ which is confined to the first Brillouin zone of the two-dimensional reciprocal lattice (lattice vectors τ). (4) shows that there exist two kinds of wave: propagating (evanescent) waves for $\kappa^2 \geqslant (<)[\boldsymbol{k}_\parallel + \tau]^2$. The number of propagating waves is finite and the number of evanescent waves infinite. Such a layer transmits and reflects an incoming wave with wave-vector $\boldsymbol{k}_\parallel$ into sets of outgoing waves on both sides of the layer. Hence, the planar scattering problem can be separated into problems which are characterized by $\boldsymbol{k}_\parallel$. In the Landauer picture this has the consequence that the reservoirs supply waves with every $\boldsymbol{k}_\parallel$ from both sides. For one $\boldsymbol{k}_\parallel$ the 'channels' are characterized by the reciprocal lattice vectors τ. For a first test of our treatment we use $\boldsymbol{k}_\parallel = \boldsymbol{0}$ (Γ point approximation). So we can use the common multichannel conductance formulas (1), (2) without modification. In the other way the conductance formulas have to be modified by replacing the summands in (1) and (2) by averages over the Brillouin zone. These two-dimensional $\boldsymbol{k}$ space integrations can be effectively done according to methods published by Cunningham and by Chadi and Cohen [9, 10].

The Γ point approximation used in this paper is particularly suitable for larger a, because for large a the size of the two-dimensional Brillouin zone is very small. That means there is a large number of propagating states (about 20–30 in our models). The position of these

reciprocal lattice vectors also depends on energy. They also vary during the energetical averaging procedure (see (6)). Despite these arguments we have to check the validity of this approximation in further calculations.

2.2. *Extraction of* ρ

To gather the resistivity of a material, we have to know how the resistance depends on the layer thickness l. If the thickness is large enough, we expect ohmic behaviour, i.e. there should be a contribution to the resistance which grows proportional to the layer thickness. Hints with respect to the minimal size of the supercell follow both from the application of the Kubo–Greenwood formula and from DOS calculations. We obtain about 100 atoms as the lower limit. Moreover, calculations on supercells with up to 3000 atoms (pure s scattering) were performed. It turned out that only a range of small layer thickness has to be excluded (see also subsection 4.1).

The conductivity can be extracted from the slope of the conductance as a function of the layer thickness. However we have to take effects into account which are not bulk typical. There is an additional contribution to the resistance R_p which comes from non-ohmic behaviour in the surface region and there are fluctuations too. So we have to fit the function

$$G_{\mathrm{Ohm}}(E) = \left(R_p(E) + \frac{l}{A\sigma(E)} \right)^{-1} \tag{5}$$

to the conductance dependence on l using a least-squares method. So the fit should begin after the surface region. In this way we extract the conductivity from the quantum mechanically defined fluctuating reflection and transmission probabilities. The result should not depend on the geometry of the sample, especially if the supercell edge a is large enough.

Note that the equations (1) and (2) define the conductance on the energy shell. At a finite temperature $T \neq 0$ we have to calculate $\sigma(E)$ for some energies around E_F, if we want to include the smoothing of the Fermi surface. The weighting procedure which calculates a temperature dependent conductivity from on the energy shell contributions is taken from the Kubo–Greenwood formula, as

$$\sigma = \int_0^\infty \mathrm{d}E \left(-\frac{\mathrm{d}f}{\mathrm{d}E} \right) \sigma(E). \tag{6}$$

For non-interacting particles this relation is true independently of the procedure which gives $\sigma(E)$. Today, to our knowledge, no well established energy averaging procedure is available which comes from the theory of multichannel conductance formulae. We treat temperature effects in the simplest way, including the smoothing of the Fermi surface. That means, we calculated $\sigma(E)$ of about 40 energy levels for the liquid systems and 20 for the amorphous one.

2.3. *The S matrix*

The layer is described by a scattering matrix $\mathcal{T}$ or a S matrix $S = \mathcal{T} + \mathcal{P}$ where $\mathcal{P}$ is the free particle propagator between the layer boundaries [7, 11]. The $S_{\tau\tau'}^{\alpha\alpha'}$ are the elements of S and describe the scattering of incident waves of channel τ', direction α' into outgoing waves channel τ and direction α (see 4). Hence, S can be subdivided into four blocks, which belong to the possible combinations of the indices α and α'.

The channels i and j in (3) have to be replaced by τ and τ', respectively, and we calculate the transmission (T_τ) and the reflection (R_τ) from the corresponding elements $\mathcal{S}^{\alpha\alpha'}_{\tau\tau'}$.

Our problem is to calculate $\mathcal{S}$ as a function of l. This can be achieved by means of the transfer matrix method [12, 13] or by S matrix methods [11, 14, 15, 16]. We have checked, analytically and numerically [8], these methods in view of our purposes. It turned out that they cannot be used for dense realistic strong d scattering systems. The reason is that many evanescent waves contribute to the interplanar multiple scattering, due to the small separation between the lattice planes. Therefore the S matrix has to be calculated in a common spherical wave based treatment. To solve the problem, we have to calculate the incident fields at each scatterer in an angular momentum representation. This is done as in LEED calculations [17, 18, 19]. The equation system for the incident fields $\Psi_L(r_j)$ at the reference scatterer at r_j in the jth lattice plane of an N_{at}-scatterer supercell system reads as

$$\Psi_L(r_j) = \Psi_L^{inc}(r_j) + \sum_{L'} f_{l'}(r_j) G'_{LL'} \Psi_{L'}(r_j) + \sum_{i \neq j}^{N_{at}} \sum_{L'} f_{l'}(r_i) G^{ji}_{LL'} \Psi_{L'}(r_i). \tag{7}$$

$\Psi_L^{inc}(r_j)$ is the primary field. The structure information is concentrated in the structure constants $G^{(ji)}_{LL'}$ and $G'_{LL'}$ which describe the inter- and intralayer propagation.

$$G^{ji}_{LL'} \equiv \sum_{\bar{L}} C(L|\bar{L}|L') G^{ji}_{\bar{L}0} = \sum_{\bar{L}} C(L'|\bar{L}|L) G^{ji}_{0\bar{L}} \tag{8}$$

$$G^{(ji)}_{0\bar{L}} = \sum_{r_s^{(s)}} i\kappa h^{(1)}_{\bar{L}}(r_j - r_s^{(i)}) \exp i\boldsymbol{k}_\parallel \cdot (r_s^{(i)} - r_i) \tag{9}$$

and

$$G'_{LL'} \equiv \sum_{\bar{L}} C(L|\bar{L}|L') G'_{\bar{L}0} = \sum_{\bar{L}} C(L'|\bar{L}|L) G'_{0\bar{L}} \tag{10}$$

$$G'_{0\bar{L}} = \sum_{r_s^{(j)} \neq r_j} i\kappa h^{(1)}_{\bar{L}}(r_j - r_s^{(j)}) \exp[i\boldsymbol{k}_\parallel \cdot (r_s^{(j)} - r_j)]. \tag{11}$$

Equation (9) is calculated in reciprocal space whereas (11) is obtained by means of an Ewald summation technique [20]. The $C(L|\bar{L}|L') = \sqrt{4\pi} \int d\Omega_{\hat{e}} Y^*_L(\hat{e}) Y_{\bar{L}}(\hat{e}) Y_{L'}(\hat{e})$ are the Gaunt coefficients. The calculation of the interlayer structure constants takes a significant part of the CPU time in numerical calculations. Once we have determined the structure constants, we can use them to calculate a scattering matrix in angular momentum representation. In a compact formulation we rewrite (7) upon introducing the diagonal matrix $\mathcal{F}$ which involves the partial scattering amplitudes $f_l(r_j)$ at each atomic site,

$$|\Psi\rangle = |\Psi^{inc}\rangle + \mathcal{G}\mathcal{F}|\Psi\rangle. \tag{12}$$

This equation for $|\Psi\rangle$ can be solved by simple matrix manipulation. To get the amplitude of the scattered wave, the vector $|\Psi\rangle$ has to be multiplied by $i\kappa\mathcal{F}$. This gives

$$|\Psi^{sc}\rangle = i\kappa[\mathcal{F}^{-1} - \mathcal{G}]^{-1}|\Psi^{inc}\rangle. \tag{13}$$

$i\kappa[\mathcal{F}^{-1} - \mathcal{G}]^{-1}$ is the scattering matrix in angular momentum representation. If we use a block notation, this matrix reads

$$[\mathcal{F}^{-1} - \mathcal{G}]^{-1} = \begin{pmatrix} \mathbf{F}_1^{-1} - \mathbf{G}' & -\mathbf{G}^{12} & \dots & -\mathbf{G}^{1N_{at}} \\ -\mathbf{G}^{21} & \mathbf{F}_2^{-1} - \mathbf{G}' & \dots & -\mathbf{G}^{2N_{at}} \\ \dots & \dots & \dots & \dots \\ -\mathbf{G}^{N_{at}1} & -\mathbf{G}^{N_{at}2} & \dots & \mathbf{F}_{N_{at}}^{-1} - \mathbf{G}' \end{pmatrix}^{-1} \tag{14}$$

where the blocks $\mathbf{G}^{ij}$ describe the interaction between lattice planes i and j while $\mathbf{G}^{l}$ describes the intralayer coupling. The elements of the $\mathbf{G}^{ij}$ and $\mathbf{G}^{l}$ blocks are defined in (9)–(11). The inversion of (14) can be performed successively. That means, if we have already inverted one block of a matrix we can include the next row and the next column of (14) and get the inverse of the new block. The procedure is based on simple matrix manipulations. Using this procedure and ordering the scatterers with increasing l, we get the scattering matrix in angular momentum representation of every number of lattice planes, that is for every layer thickness.

Equation (3) requires a representation in a plane wave basis. This is why we have to transform (13) or (14) into this basis. This can simply be done using the matrices

$$\{\mathcal{A}\}_{Lj\,\tau\alpha} = \frac{1}{\sqrt{\kappa_\tau}}\sqrt{4\pi}(-1)^m \begin{cases} \exp \mathrm{i}k_\tau^+ \cdot (r_j - r_l) Y_{-L}(\hat{k}_\tau^+) & \alpha = + \\ \exp \mathrm{i}k_\tau^+ \cdot (r_j - r_r) Y_{-L}(\hat{k}_\tau^-) & \alpha = - \end{cases} \tag{15}$$

and

$$\{\mathcal{B}\}_{\tau\alpha\,Li} = \frac{2\pi}{\kappa\sqrt{\kappa_\tau}A}\sqrt{4\pi} \begin{cases} \exp \mathrm{i}k_\tau^+ \cdot (r_r - r_i) Y_L(\hat{k}_\tau^+) & \alpha = + \\ \exp \mathrm{i}k_\tau^+ \cdot (r_l - r_i) Y_L(\hat{k}_\tau^-) & \alpha = -. \end{cases} \tag{16}$$

The matrix $\mathcal{A}$ transforms from plane wave amplitudes at reference points (r_l and r_r) on both sides of the layer into amplitudes of spherical waves at each scatterer whereas the reverse transformation is achieved by $\mathcal{B}$. So the S matrix can be written as

$$S = \mathrm{i}\kappa\mathcal{B}[\mathcal{F}^{-1} - \mathcal{G}]^{-1}\mathcal{A} + \mathcal{P} \tag{17}$$

where we used the matrix $\mathcal{P}$, which describes free propagation between the reference points. $\mathcal{P}$ is a diagonal matrix with the elements $\mathcal{P}_{\tau\tau'}^{\alpha\alpha'}(r_r - r_l) = \delta_{\alpha\alpha'}\delta_{\tau\tau'} \exp \mathrm{i}\alpha k_\tau^\alpha \cdot (r_r - r_l)$ where δ is the Kronecker symbol.

3. Input

3.1. Structure

The structure models were prepared by H Solbrig with both MC and RMC algorithms, where the experimental input data are taken from [21, 22, 23]. We examined two liquid TMs (Ni, Fe) and two amorphous TM–metalloid glasses ($Ni_{80}P_{20}$, $Fe_{80}B_{20}$). In figures 2 and 3 we show the experimental pair correlation functions in comparison with the pair correlation functions of our models of the Ni and the Ni–P system. The structures are prepared in cubic supercells with 60–120 atoms including periodic boundary conditions†. Especially for the small clusters it was not possible to produce very good agreement with experimental correlation functions because of the small number of degrees of freedom in such systems.

Table 1 shows the particle densities, temperatures and the cluster sizes of our input structures, together with the experimental references.

3.2. Scattering phase shifts

For the calculation of the S matrix the scattering amplitudes, f_l, of the effective atoms are required. The f_l are related to the partial phase shifts η_l according to $f_l = (\sin \eta_l \exp \mathrm{i}\eta_l/\kappa)$ and depend on the atomic species. Phase shifts were obtained from self-consistent DOS calculations employing the same structure models [24]. These calculations work in MS

† In the resistivity calculations we always carried out calculations on 120-atom clusters. For the small clusters therefore we fitted two clusters together to reach greater layer thickness.

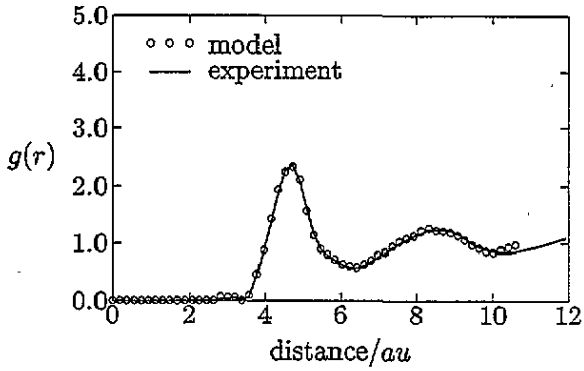

Figure 2. Comparison of the pair correlation function of one Ni model (120 atoms) with experiment.

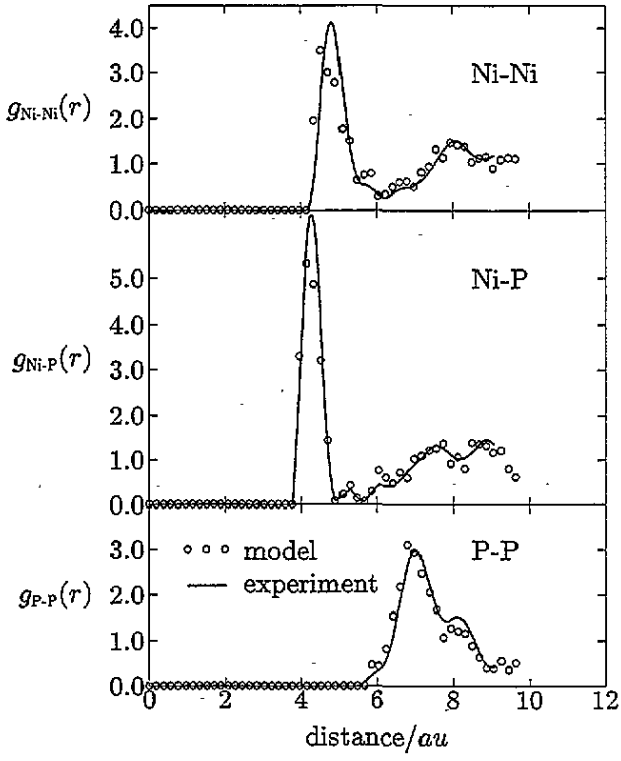

Figure 3. Partial pair correlation in the Ni–P system (of a 100-atom model) in comparison with experiment.

and LMTO formalism and were carried out by Arnold. As a starting point this serves as a reasonable approximation to the effective atom potential. With that potential a DOS calculation is performed from which we get new occupation numbers of the atomic states and a new approximation to the effective atom potential. This procedure is carried out until convergence is reached. Figures 4 and 5 show the total DOS and the phase shifts together with the Fermi levels and the resonance energies of the Ni and the $Ni_{80}P_{20}$ systems. In all systems the Fermi level lies above the d resonances in the upper DOS peak. This is why the

DOS at E_F is very sensitive to the position of E_F. Hence the transport properties are also sensitive to small variations of E_F. Close to E_F we have predominant TM d scattering. The TM s scattering as well as the scattering at the metalloid atoms have medium strengths. The TM p scattering is very weak.

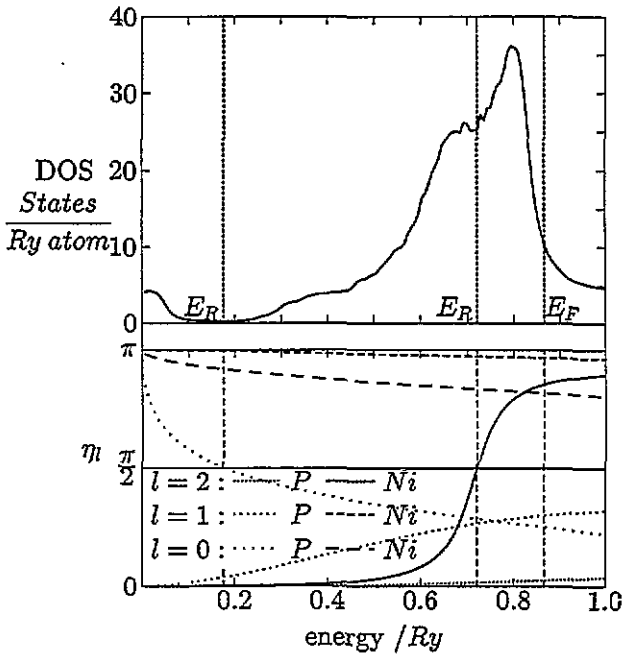

Figure 4. DOS of liquid Ni together with the partial phase shifts; E_F—Fermi level; E_R—resonance energy.

4. Results

4.1. Qualitative behaviour

For a test we applied our method to systems of s scatterers. In such a case one can calculate the S matrix upon adding successively lattice planes in plane wave representation (see above). This has the advantage that we can stack together very many lattice planes. The CPU time is proportional to the layer thickness l and the memory demand is independent of that thickness. For this check we employed clusters of liquid TMs. The s phase shifts were changed to simulate weak or strong scattering and the other phase shifts were set equal to zero. We investigated cubic supercells of 60–300 atoms.

To reach greater layer thickness, long basic cells with up to 3000 atoms were prepared upon stacking slightly modified cubical cells. It turned out that trends towards periodicity in the third direction have significant influence on the transmission through the layer, especially for weak scattering. If we wanted to do quantitative calculations on weak-scattering systems, we had to improve the structures in doing MC or RMC procedures on such long basic cells to prevent periodicity in the third dimension. On the other hand such weak-scattering systems, according to our method, need larger basic areas of the two-dimensional supercells to guarantee that the mean free path is smaller than the cell dimensions. So the model should

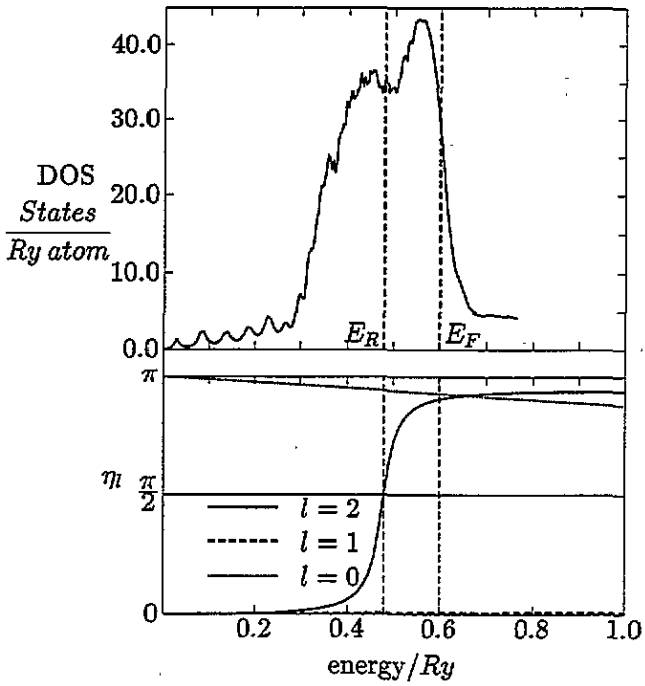

Figure 5. DOS and partial phase shifts of amorphous $Ni_{80}P_{20}$; E_F—Fermi level; E_R—resonance level.

Table 1. Data of our 11 model structures.

Material	Atom number	Supercell edge (au)	Layer thickness (au)	Temperature (K)	Particle density (au^{-3})	Exp. data
Ni	60	17.22	35.44	1773	0.011 736	[21]
	80	18.96	27.50			
	80	18.96	27.95			
	120	21.70	21.70			
Fe	60	17.50	35.00	1833	0.011 202	[21]
	80	19.26	28.57			
	120	22.04	22.04			
$Ni_{80}P_{20}$	100	19.65	23.81	300	0.013 180	[22]
	120	20.88	20.88			
$Fe_{80}B_{20}$	100	19.22	22.70	300	0.014 077	[23]
	120	20.43	20.43			

not be used for quantitative resistivity calculations in weak-scattering systems. Here we only check the accuracy of the S matrix calculation. Figure 6 shows the resistance according to (1) and (2) multiplied by the area of the two-dimensional basic cell. Note that different results for the absolute value of resistance are obtained depending on the employed formula. But the first derivative is nearly the same after the first layers†. This is also true if we compare different clusters. Figure 6 shows calculations for the smallest (60 atoms) and the largest (300 atoms) one. The qualitative behaviour is nearly the same for different choices of δ_0.

† This behaviour can be explained by the model which underlies the derivation of the different conductance formulas [7].

4.2. Application to realistic materials

If we want to treat realistic strongly scattering 3d TM systems with this method, we have to circumvent one problem: we cannot use methods that calculate the S matrix successively from plane wave S matrices. It must be calculated in the angular momentum representation (see section 2). We are numerically limited to cluster sizes of about $\approx 10^2$ atoms. In the following, all calculations will be performed with 120-atom samples (see table 1).

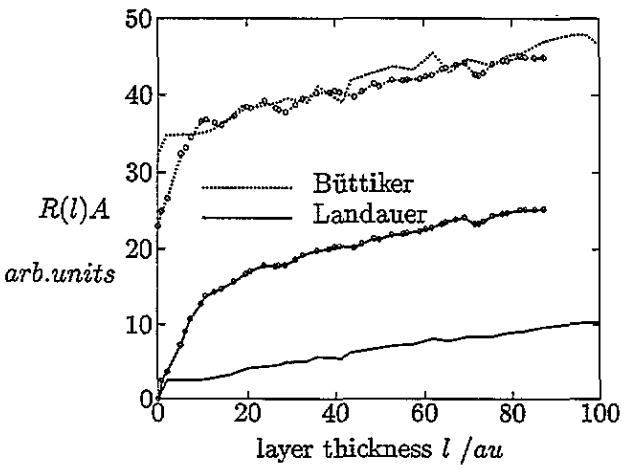

Figure 6. Resistance (defined on energy shell) as a function of layer thickness multiplied by the area of the two-dimensional basic cell for a layer build up from 60-atom clusters and 300-atom clusters (o o o) in arbitrary units.

Table 2. Comparison of calculated resistivities of the model structures from table 1 with other theoretical and with experimental results.

Material	Atom number	ρ_{calc} ($\mu\Omega$ cm)	$\rho_{calc}(E_F)$ ($\mu\Omega$ cm)	$\bar{\rho}_{calc}$ ($\mu\Omega$ cm)	ρ_{Kubo} ($\mu\Omega$ cm)	ρ_{exp} ($\mu\Omega$ cm)
Ni	60	105 ± 6	107 ± 10	104	80 [25], 170 [26]	83 [27], 85 [28]
	80	95 ± 8	102 ± 9			
	80	110 ± 5	110 ± 12			
	120	105 ± 5	103 ± 9			
Fe	60	107 ± 6	104 ± 12	106	127 [26], 180 [25]	136 [27], 137.6 [29]
	80	100 ± 4	115 ± 10			
	120	112 ± 4	116 ± 13			
$Ni_{80}P_{20}$	100	110 ± 6	111 ± 12	109	130 [30]	112 [31], 130 [32]
	120	107 ± 8	105 ± 15			132 [33]
$Fe_{80}B_{20}$	100	125 ± 12	125 ± 15	124		119 [34], 140 [35]
	120	123 ± 10	124 ± 13			

In order to demonstrate how resistance depends on the layer thickness, we present two examples in figures 7 (liquid Ni at 1773 K) and 8 (amorphous $Ni_{80}P_{20}$ at 300K) at $E = E_F$. The most important contribution to $\sigma(E)$ arises from the Fermi energy because the first derivative of the Fermi distribution ($-df/dE$) has its maximum at E_F. Besides the function $R(l)$ we show the linear fit to $R(l)$. Obviously, the slope strongly depends on the region where the fit is done. If we exclude the starting region with great deviations from

ohmic behaviour, we get variations of the order of 10% in $\sigma(E)$ and in σ, too. We have systematically varied the fitting region. The results are shown in table 2 together with the resistivities $\rho_{\text{calc}}(E_F)$ where only the contribution of the Fermi energy is considered.

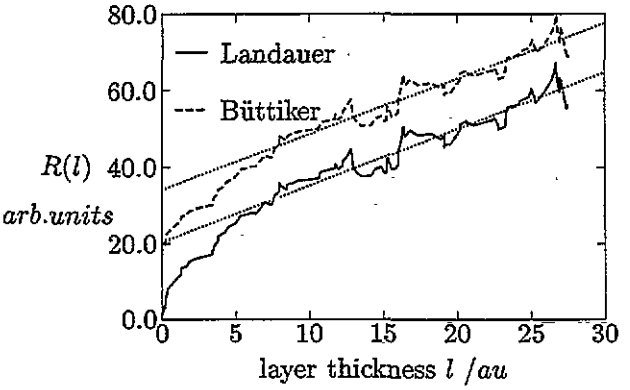

Figure 7. Liquid Ni at 1773 K. Resistance as a function of layer thickness in arbitrary units. At every energy there are large fluctuations. The fit region was 12–27 au.

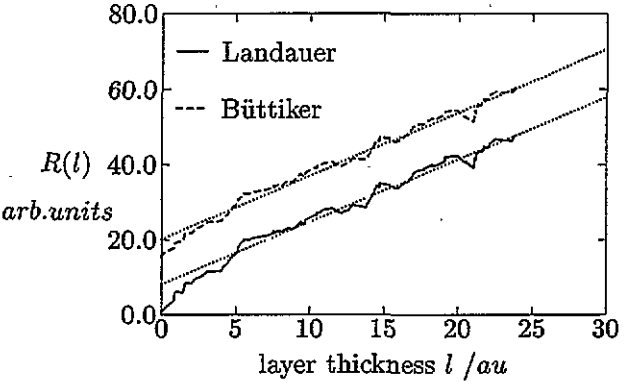

Figure 8. Amorphous $Ni_{80}P_{20}$ at 300 K. Resistance as a function of layer thickness in arbitrary units. The fluctuations are smaller than in the liquid system. The fit region was 12–23 au.

No systematic correlations of ρ_{calc} with the atom number of the basic cluster were found in our calculations. This means that our supercells are already large enough. However, many more calculations at various scattering strengths are required in order to confirm this conclusion.

If we compare our averaged values $\bar{\rho}_{\text{calc}}$ for every material with well established theoretical and experimental results, we find a very good agreement for the amorphous systems and a poorer agreement for the liquids. The theoretical results in the literature are altogether based on the evaluation of the Kubo–Greenwood formula [5]. Bose *et al* [26] did his calculations in a TB–LMTO formalism and achieved good results except for liquid Ni. The results of Asano and Yonezawa [25] are very satisfactory, too. Asano and Yonezawa as well as Yang *et al* [30] have applied a KKR method for calculating the Green function. Our calculated resistivity of liquid Ni is too high. This effect we can also see in the value given by Bose *et al* [26]. One reason could be the problems of using the density functional theory to treat this material. Another reason may be the large fluctuations of $R_{\text{Ohm}}(l)$ discussed

later in this section. They could also be responsible for the deviations in the ρ_{calc} value of liquid Fe. If we look at our results for the liquids we find deviations from experimental values of the order of 20–30%. Besides the arguments discussed above we have to mention that our method does not include inelastic scattering events which can play an important role at high temperatures†. Additionally our results are influenced by the Γ point approximation. Our best results were obtained for the amorphous materials‡. Our calculated values show deviations from the experimental values of the order 10–20%.

The behaviour of $R_{Ohm}(l)$ is significantly different for the liquid and the amorphous materials. For the liquids, this function shows greater fluctuations. The reason could be the larger variation of next-nearest-neighbour distances, especially the possibility of small distances which are the underlying cause of extremely strong multiple scattering. It may be that local self-consistency for the phase shifts is required in such cases§.

We believe that the proposed method is preferably applicable to highly resistive metallic systems‖ with $d_{at-at} \approx l_f \ll a$. For weakly scattering materials it is difficult to guarantee $a \gg l_f$.

5. Conclusions

In the Landauer/Büttiker approach the resistance of an ensemble of scatterers is derived from its transmission and reflection. This approach is commonly used to describe quantum transport phenomena. We have demonstrated that material properties like the resistivity can be obtained by this method, too. Our model system is periodic in two dimensions which gives rise to the definition of the channels. We deal with the influence of disorder in the third direction which is the transport direction. As a first approximation we confine ourselves to $k_\parallel = 0$ (Γ point). This approximation should be valid for large supercells.

The Landauer (1) and the Büttiker (2) formula differ from one another in that the latter one includes the resistance between the ideal leads and the reservoirs [7]. This is a constant part of the total resistance, R_{Ohm}. In this respect our results are very satisfying.

To obtain the resistivity we (i) calculate the fluctuating resistance as a function of the layer thickness and (ii) extract then the resistivity by linear regression. This linear fit of R_{Ohm} as a function of the layer thickness gives nearly the same results for both formulas (1) and (2). The values of R_p are different for both formulas, of course. These facts give rise to the essential statement that the resistivities obtained are almost independent of the employed formula.

The temperature is treated as in the Kubo–Greenwood formula (6) including the smoothing of the Fermi surface. Greenwood [5] has shown that (6) is true for non-interacting particles.

To test our method we calculated resistivities of realistic systems. Therefore we used realistic structure models which reproduce the experimental pair correlation functions and scattering properties which are defined self-consistently from the same structure model. The $R_{Ohm}(l)$ curves for the liquid systems show larger fluctuations than those for the amorphous systems. This causes larger variations of $\sigma(E)$ if the fitting region is moved. In forthcoming

† These effects are also neglected in the other theoretical results cited here.

‡ The experimental values of ρ from these materials fluctuate, because the samples are thin films. Their properties depend on the manufacturing conditions.

§ Our phase shifts come from self-consistently defined effective atoms (see above).

‖ We have already done calculations for liquid Ba at 1024 K and got a value of about 240 $\mu\Omega$ cm while the experimental value is 306 $\mu\Omega$ cm.

extensions our method should be able to treat thicker layers† and use local self-consistently defined scattering properties. Our hope is that we can minimize the fluctuations in this way.

Our results reproduce experimental data within 10–30% for all systems. Note that this is the first application of this method to a problem which is usually treated by the Kubo formalism. The merit of our method is that it is based on simple equations that include transmission and reflection probabilities. The resistivity is calculated in a very appealing physical picture analogous to the macroscopic meaning of resistance and resistivity.

Altogether we have shown that it is possible to use treatments established for the description of mesoscopic systems to calculate resistivities of strongly scattering systems. The present version includes full multiple scattering, based on a kind of mathematics which is common in LEED calculations. Further extensions should include Brillouin zone integrations, locally self-consistent calculations of scattering phase shifts as well as layered KKR techniques to treat thicker layers. Our hope is, that we could bring different developments in modern physics closer together. Future work will show wether our method is able to give as good results as known from applications of the Kubo–Greenwood formula.

Acknowledgments

I thank Professors H Solbrig and R Arnold for supplying all my input data and Professor R Lenk for many fruitful discussions. I also thank Dr P Lamparter and Professor S Steeb, Max-Planck-Institut Stuttgart, who have provided us with structure data. The work was financially supported by the Deutsche Forschungsgemeinschaft.

References

[1] Car R and Parrinello M 1985 *Phys. Rev. Lett.* **55** 2471
[2] Hausleitner Ch and Hafner J 1993 *Phys. Rev.* B **47** 5689
[3] Jank W, Hausleitner Ch and Hafner J 1991 *J. Phys.: Condens. Matter* **3** 4477
[4] McGreevy R L 1991 *J. Phys.: Condens. Matter* **3** F9
[5] Greenwood D A 1958 *Proc. Phys. Soc.* **71** 585
[6] Landauer R 1957 *IBM J. Res. Dev.* **1** 223
[7] Büttiker M, Imry Y, Landauer R and Pinhas S 1985 *Phys. Rev.* B **31** 6207
[8] Kahnt R 1994 Transport in topologisch ungeordneten, stark streuenden Systemen *Dissertation A* Technische Universität Chemnitz–Zwickau PF 964, 09009
[9] Cunningham S L 1974 *Phys. Rev.* B **10** 4988
[10] Chadi D J and Cohen M L 1973 *Phys. Rev.* B **8** 5747
[11] Cahay M, McLennan M and Datta S 1988 *Phys. Rev.* B **37** 10 125
[12] Pendry J B 1990 *J. Phys.: Condens. Matter* **2** 3273
[13] Pendry J B 1990 *J. Phys.: Condens. Matter* **2** 3287
[14] Cahay M, Bandyopadhyay S, Osman M A and Grubin H L 1990 *Surf. Sci.* **228** 301
[15] Datta S, Cahay M and McLennan M 1987 *Phys. Rev.* B **36** 5655
[16] Datta S 1992 *Phys. Rev.* B **45** 1347
[17] Pendry J B 1974 *Low Energy Electron Diffraction* (London: Academic)
[18] Solbrig H 1982 Beiträge zur Theorie der Beugung niederenergetischer Elektronen an Kristalloberflächen und der dabei auftretenden Barrierenresonanzen *Dissertation B* Technische Hochschule, Karl-Marx-Stadt
[19] Van Hove M A and Tong S Y 1979 *Surface Crystallography by LEED* (Berlin: Springer)
[20] Solbrig H 1982 *Phys. Status Solidi* a **72** 199
[21] Waseda Y 1980 *The Structure of Non-Crystalline Materials—Liquids and Amorphous Solids* (New York: McGraw-Hill)
[22] Lamparter P and Steeb S 1985 *Rapidly Quenched Metals V* ed S Steeb and H Warlimont (Amsterdam: Elsevier) p 459

† One way is the use of layered KKR techniques [36].

[23] Nold E, Lamparter P, Olbrich H, Rainer-Harbach G and Steeb S 1981 *Z. Naturf.* a **36** 1032
[24] Arnold R and Solbrig H 1995 *J. Non-Cryst. Solids* to be published
[25] Asano S and Yonezawa F 1980 *J. Phys. F: Met. Phys.* **10** 75
[26] Bose S K, Jepsen O and Andersen O K 1993 *Phys. Rev.* B **48** 4265
[27] Güntherodt H-J, Hauser E, Künzi H-U and Müller R 1975 *Phys. Lett.* **54A** 291
[28] Evans R, Greenwood D A and Lloyd P 1971 *Phys. Lett.* **35A** 57
[29] Van Zytvelt J B 1981 *J. Physique Coll.* **41** C8 503
[30] Yang H, Swithart J C, Nicholson D M and Brown R H 1993 *Phys. Rev.* B **47** 107
[31] Carini J P, Nagel S R, Varga L K and Schmidt T 1983 *Phys. Rev.* B **27** 7589
[32] Naugle D G 1984 *J. Phys. Chem. Solids* **45** 367
[33] Cote P J 1976 *Solid State Commun.* **18** 1311
[34] Roy R and Majumdar A K 1985 *Phys. Rev.* B **31** 2033
[35] Strom-Olsen J O, Oliver M, Altounian Z, Muir W B and Cochrane R W 1984 *J. Non-Cryst. Solids* **61 & 62** 1391
[36] MacLaren J M, Crampin S and Vvedensky D D 1989 *Phys. Rev.* B **40** 12 176